

Vortex-liquid entanglement in $\text{Bi}_2\text{Sr}_2\text{CaCu}_2\text{O}_{8+\delta}$ films in the presence of quenched disorder

L. Miu*

*Department of Physics, Johannes Gutenberg University, D-55128 Mainz, Germany
and Department of Physics, Kent State University, Kent, Ohio 44242*

G. Jakob, P. Haibach, F. Hillmer, and H. Adrian

Department of Physics, Johannes Gutenberg University, D-55128 Mainz, Germany

C. C. Almasan

Department of Physics, Kent State University, Kent, Ohio 44242

(Received 25 August 1997)

We have investigated the thermally activated behavior of the in-plane electrical resistivity of $\text{Bi}_2\text{Sr}_2\text{CaCu}_2\text{O}_{8+\delta}$ films for magnetic fields $B \leq 10^4$ G applied parallel to the c axis. The activation energy in the vortex-liquid state changes suddenly at a crossover field B_{cr} . The anisotropy reduction generated by oxygen annealing leads to the increase of the crossover field. For $B < B_{\text{cr}}$, the activation energy U is weakly magnetic-field dependent. For $B > B_{\text{cr}}$, $U(B, T) \sim (1 - T/T_{c0})/B^{1/2}$, which corresponds to an entangled vortex fluid. The observation of vortex-liquid entanglement in the presence of relevant quenched disorder is discussed in connection with the relation between the theoretically predicted entanglement length for a clean system and the collective pinning length along the field direction. Our results suggest that, in the case of a pronounced anisotropy and significant collective pinning, the entanglement field $B_E = B_{\text{cr}} \approx \Phi_0 / \gamma^2 s^2$, where s is the inter-layer spacing. [S0163-1829(98)01205-3]

I. INTRODUCTION

The unusual parameter values of layered, high-temperature superconductors (HTSC) lead to a peculiar magnetic-field-temperature (B - T) phase diagram.¹ The large thermal fluctuations smear out the mean-field superconducting transition. It is now generally accepted that there exists a true phase transition in the mixed state separating a low-temperature vortex solid from a high-temperature vortex fluid.²⁻⁵ For clean systems, this transition is first order.^{2,3} By introducing disorder, it becomes a second-order phase transition^{4,5} from a vortex solid exhibiting zero linear resistivity ρ in the limit of small transport currents I to a vortex-liquid characterized by $\rho(I \rightarrow 0) \neq 0$. The vortex-solid-vortex-liquid transition has received considerable attention in the last few years. However, many questions remain to be answered concerning the vortex-liquid phase, which, for strongly anisotropic HTSC, such as $\text{Bi}_2\text{Sr}_2\text{CaCu}_2\text{O}_{8+\delta}$ (Bi-2212), covers a large part of the B - T phase diagram. These are related to the nature of the vortex liquid, the effective dimensionality of vortices in the vortex-liquid state, the relevance of pinning, and the existence of an entangled phase.

In the present work, we discuss some of the above issues in connection with the modifications of the in-plane $\rho(T)$ dependence introduced by the change in the anisotropy and the presence of quenched disorder in Bi-2212 films in the vortex-liquid state. The characteristic quenched disorder results mainly from the random oxygen distribution. We have found relevant pinning in the vortex-liquid state, at least at low fields. For a conventional liquid, where all the characteristic times are of the same order as the thermal fluctuation time (which is always much shorter than the pinning time), such a behavior is hard to understand. However, as discussed

in Ref. 6, this becomes possible if the vortex liquid is very viscous, with a deformation time longer than the pinning time. The origin of the large deformation time seems to be the existence of high barriers associated with the thermally activated plastic motion of the vortex structure. We explain the observed change in the magnetic-field dependence of the activation energy at a crossover magnetic B_{cr} through a transition from a low-field disentangled vortex liquid to a high-field entangled vortex liquid. Our results suggest that, for strongly anisotropic HTSC in the presence of collective pinning, the entanglement field $B_E = B_{\text{cr}} \approx \Phi_0 / \gamma^2 s^2$. The appearance of an entangled vortex-liquid phase indicates that the vortex-solid-vortex-liquid transition and the layer decoupling do not take place simultaneously.⁷ Finite resistivity in the limit of small transport currents occurs at a temperature value lower than the layer decoupling temperature.

II. SAMPLE PREPARATION AND CHARACTERIZATION

Bi-2212 films, about 4000 Å thick, were prepared by a sputtering method on (100)-oriented SrTiO_3 substrates, as described in Ref. 8. We investigated an oxygenated film, Bi-2212 $_{ox}$ (which, after deposition, was maintained for 3 h at 600 °C in a 10-Torr oxygen atmosphere), and a reduced film, Bi-2212 $_{va}$ (annealed at 500 °C for 3 h “in vacuum,” i.e., 5×10^{-2} Torr oxygen). The strongly c -axis-oriented growth was confirmed by x-ray-diffraction studies, while the transmission electron microscopy analysis revealed a low density of stacking faults. The patterning of the films into a suitable four-probe structure was performed by a standard photolithographic technique, and the electrical contacts were obtained by evaporating and annealing silver. In order to diminish the influence of the inhomogeneity in the interlayer

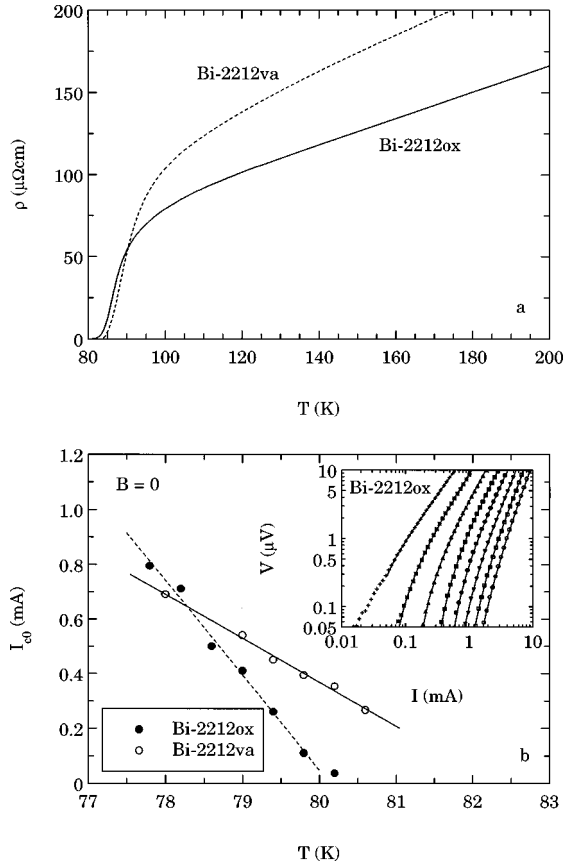


FIG. 1. (a) Zero-field resistive transitions of the investigated films for a transport current $I = 5 \mu\text{A}$. (b) Temperature dependence of the zero-field critical current I_{c0} extracted from the fit of the I - V curves as illustrated in the inset. The lines are linear fits to the data. Inset: I - V curves of the sample Bi-2212ox in zero external magnetic field fitted with the expression $V(I) \sim I(I - I_{c0})^{a-1}$ (three-parameter fit). From right to left, the temperatures was increased from 77.8 K to 80.6 K in steps of 0.4 K.

Josephson coupling across the sample, we used $0.1 \text{ mm} \times 10 \mu\text{m}$ bridges for transport measurements, with pulsed and reversed current. The electrical resistivity in the normal state of the oxygenated film is lower than that of Bi-2212va [Fig. 1(a)]. The mean-field transition temperature in zero applied magnetic field, approximated by the temperature value corresponding to the inflection point in the $\rho(T)$ dependence, is $T_{c0} \approx 88.5 \text{ K}$ for Bi-2212va and $\approx 86 \text{ K}$ for the oxygen-annealed film. The carrier concentration, as determined from the Hall constant measured at 150 K, is $\approx 15\%$ higher for the Bi-2212ox sample. All these results indicate a higher doping level for the Bi-2212ox film. It is worth noting that the degree of disorder is more pronounced in the reduced film. This is supported by the increase of the normal-state resistivity relative to that of Bi-2212ox, which is higher than the one expected to result from doping only, and by the transition width, which is larger by $\approx 1 \text{ K}$ than in the case of Bi-2212ox.

For the discussion below, it is important to know at least the relative increase of the anisotropy parameter γ after oxygen annealing. [$\gamma = (M/m)^{1/2}$, where m and M are the effective masses of the quasiparticles moving in the (a,b) plane and perpendicular to it, respectively.] This can be obtained by analyzing the temperature dependence of the critical cur-

rent in zero external magnetic field. As known, the occurrence of dissipation in highly anisotropic HTSC in zero applied magnetic field is due to the current-induced unbinding of thermally excited vortex pairs (see, for example, Ref. 9). The presence of interlayer Josephson coupling between the superconducting layers gives rise to a finite zero-field critical current I_{c0} . This is because a minimum current is needed to overcome the in-plane vortex-antivortex attraction generated by the Josephson coupling. At high temperatures, this intrinsic critical current is expected to be larger than the critical current resulting from the pinning of the thermally excited vortices. The current-voltage (I - V) characteristics are of the form^{10,11} $V \sim I(I - I_{c0})^{a-1}$, where the exponent a is the same as in the two-dimensional case. Not very close to the resistive transition, corresponding to the occurrence of finite resistivity in the limit of small transport currents, the $I_{c0}(T)$ dependence is linear and the slope $dI_{c0}/dT \sim 1/\gamma$.¹⁰ The zero-field I - V curves of the two samples were fitted with the above equation in a three-parameter fit, as illustrated in the inset to Fig. 1(b) for the Bi-2212ox sample. Here we are interested in the I_{c0} values only. The temperature dependence of the critical current obtained from the fit is plotted in Fig. 1(b). The change in the slope of $I_{c0}(T)$ indicates that the anisotropy parameter of the oxygen-annealed sample is by a factor of 2.2 smaller than that of the vacuum-annealed specimen. The zero-field critical current vanishes at a temperature value lower than T_{c0} due to the occurrence of a vortex-fluctuation induced layer decoupling.¹¹

III. RESULTS AND DISCUSSION

As reported earlier,¹²⁻¹⁵ the temperature dependence of the in-plane resistivity of Bi-2212 single crystals and thin films in a magnetic field applied along the c axis is well described, at low resistivity levels, by the thermally activated form

$$\rho(B, T) = \rho_0 \exp[-U(B, T)/T], \quad (1)$$

where $U(B, T)$ is the activation energy ($k_B = 1$). The results of the present analysis remain essentially the same when the factor ρ_0 from Eq. (1) is approximated by the sample resistivity in the normal state, at $T = 120 \text{ K}$, for example, or by the sample resistivity at T_{c0} . Equation (1) and the Ohmic resistivity at small transport currents are explained in terms of thermally assisted flux flow.¹⁶ The Arrhenius plots of the reduced resistivity $\rho(T)/\rho(120 \text{ K})$ for the vacuum-annealed film, at a transport current of $5 \mu\text{A}$, are illustrated in Fig. 2. By varying the transport current within three orders of magnitude, the Arrhenius plots do not change, which is characteristic for a vortex-liquid phase. The strong reduction of the resistivity with decreasing temperature (compared with the behavior of the flux flow resistivity) suggests that the quenched disorder remains relevant for the vortex-fluid phase as well, at least at low applied fields.

In the sensitivity window of our measurements, the Arrhenius plots of the reduced resistivity are linear at low resistivity levels (Fig. 2), which means that the activation energy has a linear temperature dependence. One can determine the activation energy $U(T)$ directly, from the resistive

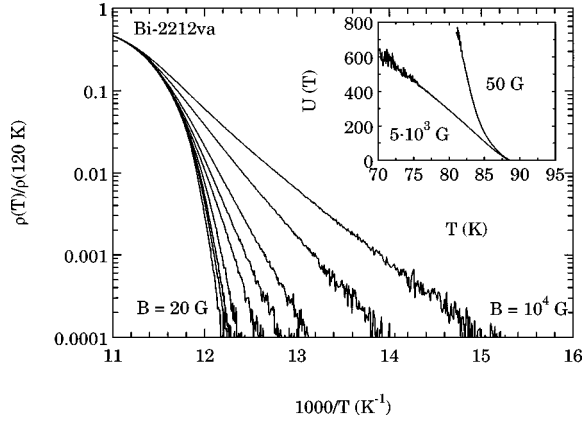


FIG. 2. Arrhenius plots of the reduced resistivity in magnetic fields applied parallel to the c axis for the sample Bi-2212va (the transport current was of $5 \mu\text{A}$). B (G) = 20, 50, 100, 200, 500, 5×10^3 , 10^4 . Inset: Temperature dependence of the activation energy U at low fields, $B = 50$ G, and at high fields, $B = 5$ kG (sample Bi-2212va).

data for constant B , using Eq. (1) and making the natural assumption that $U(T)$ vanishes at T_{c0} : $U(T) = T\{\ln[\rho(T_{c0})] - \ln[\rho(T)]\}$. The inset to Fig. 2 illustrates that, at high-field values and not very close to T_{c0} , the activation energy is very well described by the relation $U(B, T) = U_0(B)(1 - T/T_{c0})$. For low fields, the $U(T)$ variation is modified by the occurrence of a vortex-fluctuation-induced layer decoupling at high temperatures¹⁷⁻¹⁹ and the possible transition to a vortex glass at lower temperatures.^{4,5} However, for a limited resistivity interval, at low resistivity levels (in the sensitivity window of our measurements), the $U(B, T)$ dependence can be considered of the form $U(B, T) = U_0(B)(1 - T/T^*)$, with $T^* < T_{c0}$.

Figure 2 suggests that, for low fields, the activation energy has a weak magnetic-field dependence, in contrast to the behavior at high fields. To show this, we determined the activation energy U_0 as the slope in the Arrhenius plot for $\rho(B, T)/\rho(120 \text{ K})$ between 10^{-3} and 10^{-4} . In the low-field region, the activation energy extracted this way is approximately 30% larger for Bi-2212va (7×10^3 K at $B = 20$ G), which confirms the fact that, at least not far away from the isolated vortex limit, the quenched disorder is relevant. In order to minimize the influence of a different degree of disorder on $U_0(B)$, the activation energy was normalized to its value at 20 G. Figure 3 illustrates the field dependence of the reduced activation energy $U_{\text{red}}(B) = U_0(B)/U_0(20 \text{ G})$. The notable feature is the sudden change of the magnetic-field dependence of the activation energy at $B_{\text{cr}} \approx 300$ G for the sample Bi-2212va and at $B_{\text{cr}} \approx 1400$ G for Bi-2212ox.

The modification of $U_0(B)$ must be reflected in the shape of the “resistive irreversibility line,” determined in the vortex-liquid state, with a finite resistivity criterion.²⁰ For example, we defined the “irreversibility temperature” T_R as the temperature value where $\rho(T_R)/\rho(120 \text{ K}) = 10^{-4}$. The resulting $T_R(B)$ line is shown in Fig. 4. The $T_R(B)$ variation changes its form basically at the same field B_{cr} (see Figs. 3 and 4). One may think that, due to the relatively low B_{cr} values in the case of highly anisotropic samples, the change of the resistive irreversibility line, as illustrated in Fig. 4, is the result of the disintegration of the vortex lines in a system

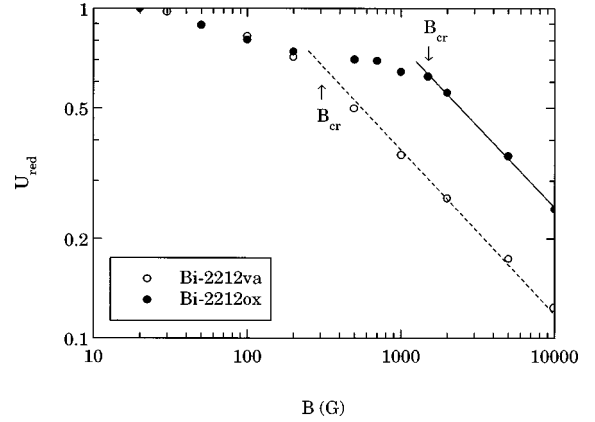


FIG. 3. Magnetic-field dependence of the reduced activation energy $U_{\text{red}} = U_0(B)/U_0(20 \text{ G})$, where U_0 was determined as the slope in the Arrhenius plots for $10^{-3} \leq \rho(T)/\rho(120 \text{ K}) \leq 10^{-4}$. The lines are fits of $U_{\text{red}}(B)$ for $B > B_{\text{cr}}$ with the function $U_{\text{red}}(B) = \text{const} \times B^{-1/2}$.

of decoupled superconducting layers.¹⁷ This is expected to occur for isolated vortex lines, above a temperature value T_d corresponding to the decoupling of the superconducting layers induced by thermally excited vortices and antivortices.¹⁸ However, the analysis of the zero-field $\rho(T)$ dependence in the framework of the Coulomb gas model²¹ gives for the sample Bi-2212ox $T_d \geq 81$ K,²² which is larger than any $T_R(B)$ value for a resistive criterion smaller than 10^{-3} .

For $B < B_{\text{cr}}$, the activation energy varies slowly with B , as expected close to the isolated vortex limit. For $B > B_{\text{cr}}$, the activation energy is proportional to $B^{-1/2}$ (Fig. 3). An activation energy of the form $U(B, T) \sim (1 - T/T_{c0})/B^{1/2}$ is characteristic for cutting and reconnection of vortices, which appear in the case of the thermally activated plastic motion of an entangled vortex liquid. The size of the characteristic plastic barriers has been estimated in Refs. 6 and 23. The basic idea is that the relevant excitations involve deformations of vortices on a scale of the order of the mean inter-vortex separation, giving rise to an activation energy

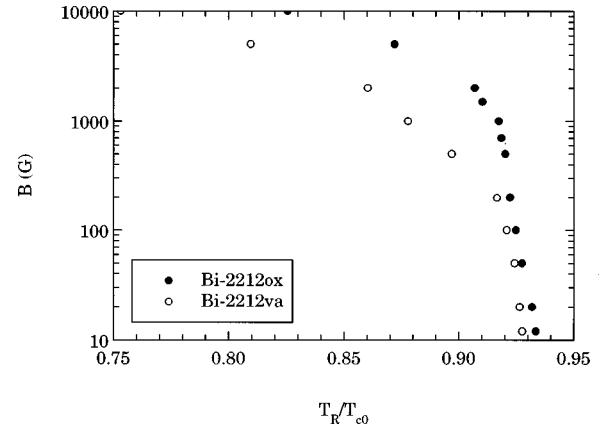


FIG. 4. “Resistive irreversibility line” of the investigated samples determined with a low resistivity criterion, $\rho(T_R)/\rho(120 \text{ K}) = 10^{-4}$. The shape of this line changes basically at the same B_{cr} value where the magnetic-field dependence of the activation energy modifies.

$$\begin{aligned}
U(B, T) &\approx \Phi_0^{5/2} (1 - T/T_{c0}) / [8\pi^2 \gamma \lambda^2(0) B^{1/2}] \\
&= U_0(B) (1 - T/T_{c0}), \quad (2)
\end{aligned}$$

where $\lambda(T) = \lambda(0)(1 - T/T_{c0})^{-1/2}$ is the in-plane component of the magnetic penetration depth. For $B > B_{cr}$, the decrease of the anisotropy parameter induced by oxygen annealing, as determined in Sec. II, and the data from Fig. 3 show that $U_0(B) \sim 1/\gamma$, in agreement with Eq. (2). With U_0 of the order of 10^3 K at $B = 10^4$ G for the oxygen-annealed sample and $\lambda(0) = 1500$ Å, Eq. (2) gives $\gamma \approx 10^2$. The data from Fig. 3 also indicate that $B_{cr} \sim 1/\gamma^2$.

We associate the modification of the $U_0(B)$ dependence at $B = B_{cr}$ with a transition from a disentangled to an entangled vortex fluid in the presence of collective pinning. A transition from the Meissner state to an entangled vortex liquid was theoretically predicted in Ref. 24 in the absence of relevant disorder. In a clean system, once the vortices in the liquid wander a distance equal to the mean intervortex spacing, the vortex assemble becomes entangled, in the sense that its dynamic behavior will be strongly influenced by the barriers to vortex cutting and reconnection. The entanglement length L_E , representing the length along the field direction required for the vortex lines to wander a distance equal to the mean intervortex separation, can be obtained from the analogy between the entangled vortex liquid and the superfluid ground state of a system of two-dimensional bosons.^{1,24} This leads, for a diluted vortex liquid, to $L_E(T) \approx \Phi_0 \varepsilon_0 \ln \kappa / 2\pi \gamma^2 k_B T B$, where the energy scale $\varepsilon_0 = (\Phi_0 / 4\pi \lambda)^2$, and κ is the Ginzburg-Landau parameter (of the order of 10^2). In the absence of notable pinning, one reaches the entanglement field B_E when the entanglement length equals the sample thickness. However, in the presence of relevant disorder, as in the case of our thin-film samples, the dynamic response corresponding to the plastic motion of the entangled vortex liquid will be seen only if the entanglement length becomes at least equal to the collective pinning length L_c .¹ The high values of the activation energy determined for our samples at low fields indicate that the collective pinning length can be much smaller than the film thickness. In the isolated vortex limit, L_c can be estimated from the collective pinning energy $U_c \approx T_{c0} \text{Gi}^{-1/2} \xi / L_c$, where $\xi(T) = \xi(0)(1 - T/T_{c0})^{-1/2}$ is the in-plane coherence length and Gi is the Ginzburg number.¹ [For Bi-2212, $\xi(0) \approx 20$ Å, and $\text{Gi} \approx 0.1$.²⁵] At low fields, with $U_c \approx U(B, T) \approx 600$ K (see Fig. 2, inset), the above relation gives $L_c \approx 30$ Å. By taking into account the anisotropy, L_c can be even lower.²⁶ In the condition of relevant disorder, the dominant effect at low fields (where $L_c \ll L_E$) is the pinning of individual vortices by the disordered potential. The boundary between the collective pinning response and the thermally activated plastic motion of the entangled vortex liquid is then fixed by the condition $L_E \approx L_c$, and the corresponding entanglement field would be

$$B_E = \Phi_0 \varepsilon_0 \ln \kappa / 2\pi \gamma^2 k_B T L_c. \quad (3)$$

With the above estimate for L_c and $\lambda(0) \approx 1500$ Å, Eq. (3) gives an entanglement field value which is approximately one order of magnitude higher than B_{cr} , if one takes $\kappa \approx \gamma \approx 10^2$. [For $B > \Phi_0 / \lambda^2$, the intervortex interaction should be taken into account, and the line tension $\varepsilon_0 \ln \kappa$ in Eq. (3) must

be accordingly replaced by the appropriate tilt modulus, but this would lead to a larger entanglement field.]

The observation of vortex-liquid entanglement in Bi-2212 thin films at fields much lower than the B_E value predicted by Eq. (3) may have its origin in a particular evolution of the entanglement length with the flux density in the case of highly anisotropic HTSC. As discussed in a number of theoretical studies,^{26–29} in the case of a pronounced anisotropy, the vortices are very sensitive to the discreteness of the layered structure. At high enough temperatures, the thermal fluctuations can cause the decomposition of vortex lines into pancake vortices located in the superconducting layers. In our situation, the wandering of these vortex segments in the superconducting layers seems to be the dominant process. The wandering distance can easily attain the mean intervortex separation, as soon as the latter is lower than the Josephson length $\lambda_J = \gamma s$. This can be understood if one represents such a vortex distortion by a straight vortex-line (string) and an additional vortex-antivortex pair, where the antivortex annihilates the vortex segment in the corresponding plane.^{17,28,29} The contribution of the interlayer Josephson coupling to the vortex-antivortex interaction is small when the vortex-antivortex separation (i.e., the vortex line deformation) is lower than λ_J .^{26–29,1} This means that L_E becomes rapidly of the order of the interlayer spacing (approaching L_c), as the mean vortex separation decreases below λ_J . The entanglement field can then be the field value for which the mean intervortex separation equals the Josephson length, which leads to

$$B_E = B_{cr} \approx \Phi_0 / \gamma^2 s^2. \quad (4)$$

In the case of the sample Bi-2212*ox*, for example, with $\gamma \approx 10^2$ and $s = 15$ Å, Eq. (4) gives an entanglement field very close to the experimentally determined B_{cr} . Finally, it is worth noting that the disorder becomes less important for an entangled vortex liquid (see Fig. 3). This is supported by the renormalization-group calculations from Ref. 30, showing that the effective coupling to the random potential is weak as long as L_E is lower than L_c .

IV. CONCLUSIONS

The analysis of the in-plane $\rho(T)$ dependence of highly anisotropic Bi-2212 films in a magnetic field applied parallel to the c axis revealed significant pinning of a disentangled vortex liquid at low fields, and a transition to an entangled vortex liquid appearing above a crossover field B_{cr} . The entanglement of the vortex liquid is suggested by the specific magnetic-field and temperature dependence of the activation energy, which becomes $U(B, T) \sim (1 - T/T_{c0})/B^{1/2}$ for $B > B_{cr}$. The existence of an entangled vortex-liquid phase implies that the vortex-solid–vortex-liquid transition temperature is lower than the layer decoupling temperature. We have found that, in the presence of significant collective pinning (with the collective pinning length along the field direction much smaller than the entanglement length predicted at low fields for a clean system), the entanglement of vortices can be observed above the field $B_E = B_{cr} \approx \Phi_0 / \gamma^2 s^2$. There is a good quantitative agreement between the increase of the entanglement field and the enhancement of the interlayer Josephson coupling generated by doping, derived from the

change of the temperature dependence of the critical current in zero external magnetic field.

ACKNOWLEDGMENTS

This project has been funded at KSU by the National Research Council under the Collaboration in Basic Science

and Engineering Program, and by the National Science Foundation under Grant No. DMR-9601839, and at the Johannes Gutenberg University by the Deutsche Forschungsgemeinschaft through Sonderforschungsbereich 262. L.M. wishes to acknowledge the kind assistance of the Alexander von Humboldt Foundation.

-
- *Permanent address: Institute for Materials Physics, P. O. Box MG-7, Bucharest, Romania.
- ¹G. Blatter, M. G. Feigel'man, V. B. Geshkenbein, A. I. Larkin, and V. M. Vinokur, *Rev. Mod. Phys.* **66**, 1125 (1994), and references therein.
 - ²H. Safar, P. L. Gammel, D. A. Huse, D. J. Bishop, J. P. Rice, and D. M. Ginsberg, *Phys. Rev. Lett.* **69**, 824 (1992).
 - ³H. Pastoriza, M. F. Goffman, A. Arribère, and F. de la Cruz, *Phys. Rev. Lett.* **72**, 2951 (1994).
 - ⁴D. S. Fisher, M. P. A. Fisher, and D. A. Huse, *Phys. Rev. B* **43**, 130 (1991).
 - ⁵R. H. Koch, V. Foglietti, W. J. Gallagher, G. Koren, A. Gupta, and M. P. A. Fisher, *Phys. Rev. Lett.* **63**, 1511 (1989); P. L. Gammel, L. F. Schneemeyer, and D. J. Bishop, *ibid.* **66**, 953 (1991).
 - ⁶V. M. Vinokur, M. V. Feigel'man, V. B. Geshkenbein, and A. I. Larkin, *Phys. Rev. Lett.* **65**, 259 (1990).
 - ⁷R. A. Doyle, D. Liney, W. S. Seow, A. M. Campbell, and K. Kadowaki, *Phys. Rev. Lett.* **75**, 4520 (1995).
 - ⁸P. Wagner, F. Hillmer, U. Frey, H. Adrian, T. Steinborn, L. Ranno, A. Elschner, I. Heyvaert, and Y. Bruynseraede, *Physica C* **215**, 123 (1993).
 - ⁹L. I. Glazman and A. E. Koshelev, *Zh. Eksp. Teor. Fiz.* **97**, 1371 (1990) [*Sov. Phys. JETP* **70**, 774 (1990)].
 - ¹⁰H. J. Jensen and P. Minnhagen, *Phys. Rev. Lett.* **66**, 1630 (1991).
 - ¹¹L. Miu, P. Wagner, U. Frey, A. Hadish, D. Miu, and H. Adrian, *Phys. Rev. B* **52**, 4553 (1995).
 - ¹²T. T. M. Palstra, B. Batlogg, L. F. Schneemeyer, and J. W. Waszczak, *Phys. Rev. B* **43**, 3756 (1991).
 - ¹³J. T. Kucera, T. P. Orlando, G. Virshup, and J. N. Eckstein, *Phys. Rev. B* **46**, 11 004 (1992).
 - ¹⁴P. Wagner, F. Hillmer, U. Frey, and H. Adrian, *Phys. Rev. B* **49**, 13 184 (1994).
 - ¹⁵T. Tsuboi, T. Hanaguri, and A. Maeda, *Phys. Rev. B* **55**, R8709 (1997).
 - ¹⁶P. H. Kes, J. Aarts, J. van den Berg, C. J. van der Beek, and J. A. Mydosh, *Supercond. Sci. Technol.* **1**, 242 (1989).
 - ¹⁷K. H. Fischer, *Physica C* **210**, 179 (1993), and references therein.
 - ¹⁸S. W. Pierson, *Phys. Rev. B* **54**, 688 (1996).
 - ¹⁹H. Weber and H. J. Jensen, *Phys. Rev. B* **44**, 454 (1991); P. Minnhagen and P. Olsson, *ibid.* **44**, 4503 (1991).
 - ²⁰L. Miu, P. Wagner, A. Hadish, F. Hillmer, and H. Adrian, *Physica C* **234**, 249 (1994).
 - ²¹P. Minnhagen, *Rev. Mod. Phys.* **59**, 1001 (1987).
 - ²²L. Miu *et al.* (unpublished).
 - ²³V. B. Geshkenbein, A. I. Larkin, M. V. Feigel'man, and V. M. Vinokur, *Physica C* **162-164**, 239 (1989).
 - ²⁴D. R. Nelson and H. S. Seung, *Phys. Rev. B* **39**, 9153 (1989).
 - ²⁵D. V. Livanov, G. Balestrino, and M. Montuori, *Physica C* **226**, 320 (1994).
 - ²⁶V. M. Vinokur, P. H. Kes, and A. E. Koshelev, *Physica C* **168**, 29 (1990).
 - ²⁷L. I. Glazman and A. E. Koshelev, *Phys. Rev. B* **43**, 2835 (1991); M. V. Feigel'man, V. B. Geshkenbein, and A. I. Larkin, *Physica C* **167**, 177 (1990); J. R. Clem, *Phys. Rev. B* **43**, 7837 (1991); L. L. Daemen, L. N. Bulaevskii, M. P. Maley, and J. Y. Coulter, *Phys. Rev. Lett.* **70**, 1167 (1993).
 - ²⁸S. N. Artemenko and A. N. Kruglov, *Phys. Lett. A* **143**, 485 (1990).
 - ²⁹K. H. Fischer, *Physica C* **178**, 161 (1991).
 - ³⁰D. R. Nelson and P. Le Doussal, *Phys. Rev. B* **42**, 10 113 (1990).